Pictorial Essay

Three-Dimensional Volumetric Display of the Nasal Ostiomeatal Channels and Paranasal Sinuses

T. F. Gotwald[1], S. J. Zinreich[2], F. Corl[3], E. K. Fishman[3]

The premise behind functional endoscopic sinus surgery is the reduction of sinus disease through improved ventilation and mucociliary clearance within the paranasal sinuses [1]. The surgical procedure is guided by endoscopy and, therefore, requires a precise understanding of the highly individualized anatomy of this area. CT in the coronal plane provides the closest imaging correlation to the endoscopist's view and has been used since the introduction of functional endoscopic sinus surgery to guide the surgeon performing this procedure [2]. Nevertheless, since the introduction of this technique, the radiologist's aim and the otolaryngologist's wish have been to view this area three-dimensionally. Given the three-dimensional (3D) reconstruction programs available over the past 15 years, an accurate 3D reconstruction of the underlying anatomy has been virtually impossible. The newly available volumetric 3D display made possible by the Virtuoso 3D workstation (Siemens Medical, Iselin, NJ) is, for the first time, able to provide reliable and realistic 3D images in an interactive, real-time display [3, 4]. The objective of this presentation is to show the 3D anatomy of the nasal cavity and paranasal sinuses with the Virtuoso 3D imaging workstation.

The Role of Imaging in Functional Endoscopic Sinus Surgery

The wide individual variability of the anatomy of the nasal cavity and paranasal sinuses; the proximity to the orbit, optic canal, and intracranial compartments; and the hidden nature of superimposed layers of cells necessitate an accurate and dependable anatomic road map to guide the surgical procedure. CT excellently displays the bony architecture and its mucosal covering as well as the narrow air channels of the ostiomeatal complex. Furthermore, CT accurately depicts the boundaries between the paranasal sinuses, the orbit, and the intracranial compartment and the relationship between the optic nerve, the cavernous carotid artery, and the fifth cranial and vidian nerves to the sphenoidal sinus [5–7].

Subjects and Methods

Patients were scanned in the axial plane (2-mm slice thickness, 1-mm reconstruction interval) on a conventional helical CT scanner (Somatom Plus 4; Siemens Medical). The imaging data were subsequently transferred to the Virtuoso 3D workstation for imaging.

The Anterior Ostiomeatal Channels

The frontal recess (Figs. 1A and 1B) is an hourglass-shaped channel affording communication between the frontal sinus and the anterior ethmoidal sinus. The frontal recess is not a tubular structure, as the former term "nasofrontal duct" implies; therefore, this term has been replaced with the term "frontal recess." The agger nasi cells (Fig. 1C), frontal cells, and suprabullar recess cells are in contiguity with the frontal recess, and the various shapes and sizes of these cells influence the patency of the frontal recess. The agger nasi cells (Fig. 2) are situated below the frontal sinus; these cells are the most anterior cells in the anterior ethmoidal sinus complex and are aerated to various degrees in virtually everyone. The agger nasi cells border the nasal bone anteriorly and the middle turbinate medially, and the uncinate process adheres to their lateral border. Supraorbital ethmoidal cells develop as an extension from the frontal or suprabullar recess. They can pneumatize the orbital plate of the frontal bone. The number and shape of cells that may be present between the agger nasi cells and the frontal sinus vary. Some frontal cells will indent and some will actually be within the perimeter of the frontal sinus. Schaeffer [8] and Van Alyea [9] describe four types of frontal cells that may encroach on the frontal sinus or frontal recess. The frontal recess affords mucociliary drainage of the frontal and anterior ethmoidal sinuses to the middle meatus and ethmoidal infundibulum. From the frontal recess, mucous may flow directly into the middle meatus medial to the uncinate process, into the ethmoidal infundibulum more laterally, or above the ethmoid bulla more posteriorly (Fig. 3). The middle meatus is an air space lateral to the middle turbinate and medial to the uncinate process and ethmoid bulla. The uncinate process is a superior extension of the medial maxillary sinus wall. Anteriorly, the uncinate process fuses with the agger nasi cells and the posterior wall of the nasal

Received February 14, 2000; accepted after revision June 1, 2000.

[1]Radiology II, University Clinic of Innsbruck, Anichstra. 35, 6020 Innsbruck, Austria.

[2]Department of Radiology, Division of Neuroradiology, Johns Hopkins Medical Institutions, Phipps B-100, 600 N. Wolfe St., Baltimore, MD 21287. Address correspondence to S. J. Zinreich.

[3]Department of Radiology, Johns Hopkins Medical Institutions, 601 N. Caroline St., Baltimore, MD 21287.

AJR 2001;176:241–245 0361–803X/01/1761–241 © American Roentgen Ray Society

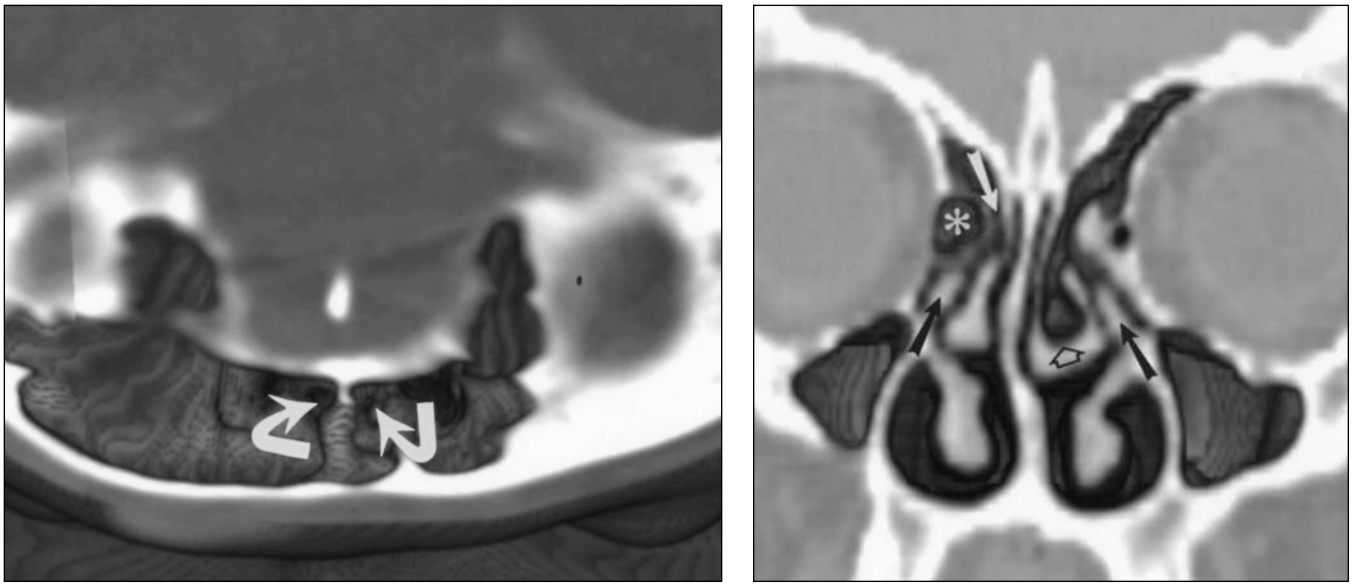

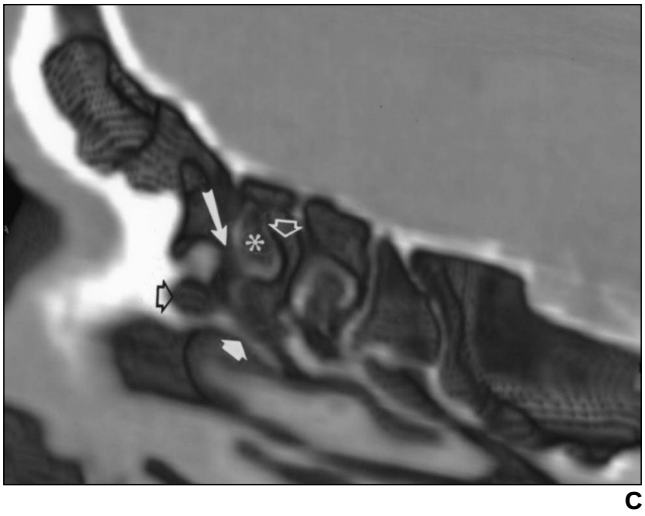

Fig. 1.—Three-dimensional volume-rendered images illustrate anatomy of frontal sinus and frontal recess region.
A, 21-year-old woman with chronic sinus pain. Axial image from helical CT data reveals frontal sinus ostia (*arrows*).
B, 33-year-old man with facial pain. Coronal image shows frontal recess (*solid white arrow*), ethmoid bulla (*asterisk*), uncinate process (*black arrows*), and concha bullosa (*open arrow*).
C, 21-year-old woman with chronic sinus pain. Sagittal image shows frontal recess (*long solid arrow*), ethmoid bulla (*asterisk*), uncinate process (*short solid arrow*), retrobullar recess (*open white arrow*), and agger nasi cell (*open black arrow*).

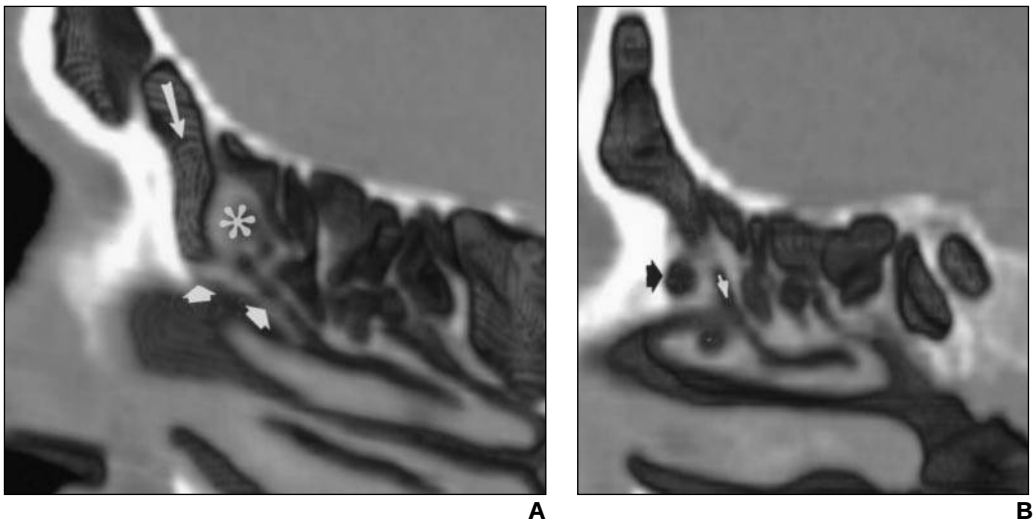

Fig. 2.—Three-dimensional volume-rendered images illustrate anatomy of anterior ethmoidal sinus region.
A, 21-year-old woman with sinus pain. Sagittal image reveals location of frontal recess (*long arrow*), ethmoid bulla (*asterisk*), and uncinate process (*short arrows*).
B, 17-year-old boy with chronic sinus pain. Sagittal image shows middle meatus, ethmoidal infundibulum (*white arrow*), and agger nasi cell (*black arrow*).

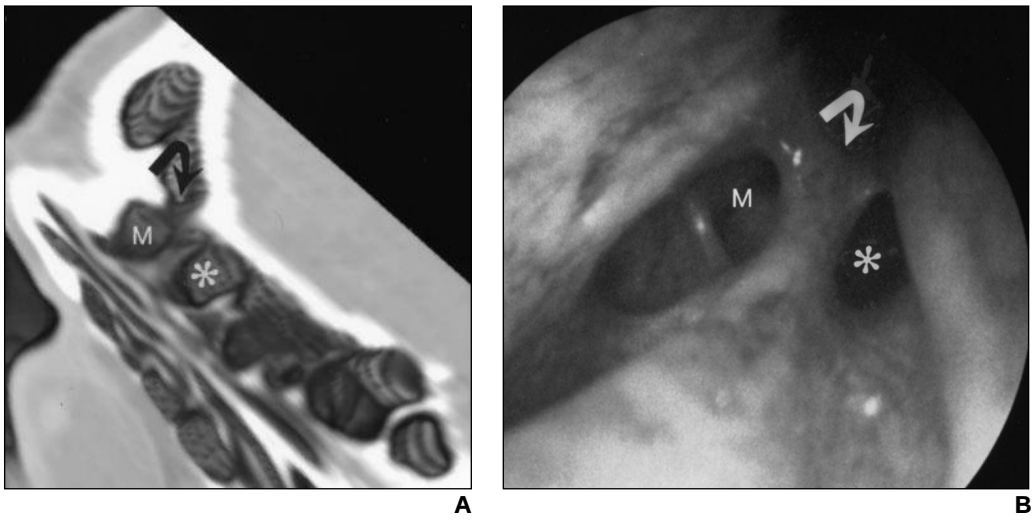

Fig. 3.—44-year-old man with chronic sinus pain.
A, Axial and sagittal three-dimensional volume-rendered image shows frontal recess (*arrow*), anterior middle meatus (M), and suprabullar recess (*asterisk*).
B, Conventional endoscopic image shows structures similar to those seen in **A**: frontal recess (*arrow*), anterior middle meatus (M), and suprabullar recess (*asterisk*).

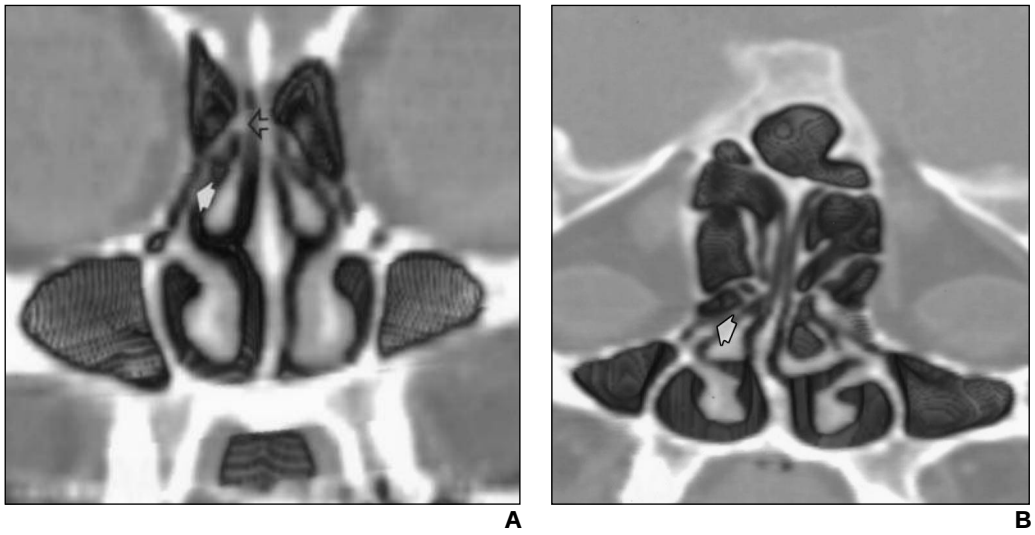

Fig. 4.—Three-dimensional volume-rendered images illustrate anatomy of uncinate process region.
A, 27-year-old man with facial pain. Coronal image reveals uncinate process (*solid arrow*) adhering to middle turbinate (*open arrow*).
B, 18-year-old woman with sinus pain. Oblique axial image shows uncinate process (*arrow*) adhering to medial wall of ethmoid bulla.

lacrimal duct. The uncinate process may adhere to the middle turbinate and to the ethmoid bulla (Fig. 4). Superoposteriorly, it has a free edge that is separated from the ethmoid bulla by a crevice termed the "inferior hiatus semilunaris." Inferiorly and laterally, this crevice communicates with the ethmoidal infundibulum, an air space bordered medially by the uncinate process and laterally by the lamina papyracea.

The ethmoidal infundibulum (Fig. 5) is an extension of the primary ostium of the maxillary sinus. Thus, ventilation and physiologic mucociliary clearance occur through the primary ostium of the maxillary sinus, into the ethmoidal infundibulum through the hiatus semilunaris inferior into the middle meatus. The ethmoid bulla is usually the largest aerated cell in the anterior ethmoidal sinus complex. Laterally, the wall of the ethmoid bulla is the

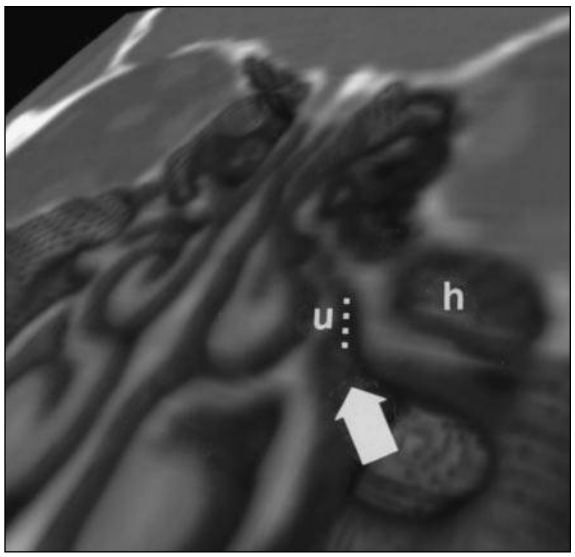

Fig. 5.—32-year-old man with sinus pain. Oblique coronal three-dimensional volume-rendered image reveals primary ostium of maxillary sinus (*arrow*), uncinate process (u), ethmoidal infundibulum (*dotted line*), and infraorbital recess cell (h).

lamina papyracea. In most patients, the ethmoid bulla is totally enclosed with only a small ostium present; however, occasionally the posterior wall of the ethmoid bulla is absent whereby the ethmoid bulla and retrobullar recess (sinus lateralis) are a single air space. The retrobullar recess is the most posterior air space in the anterior ethmoidal sinus complex.

The middle turbinate adheres anteriorly and superiorly to the skull base just lateral to the cribriform plate. It fuses together anteriorly with the uncinate process and the medial wall of the agger nasi cell. As the middle turbinate projects posteriorly, it is located medial to the structures mentioned earlier and provides the medial border for the middle meatus. Approximately in its mid course, "leaflets" begin to fan out, attaching laterally to the lamina papyracea and posteriorly to the roof of the ethmoidal sinus. The first lateral attachment is the basal lamella, which forms the boundary between the anterior and posterior ethmoidal sinus complex (Fig. 6).

The Posterior Ostiomeatal Channels

The relationship between the aerated portion of the sphenoidal sinus and the posterior ethmoidal sinus needs to be accurately perceived by the surgeon to avoid complications during surgery. This morphology is best displayed in the axial plane with 3D imaging (Fig. 7) of the sphenoidal sinus.

Usually in the paramedian sagittal plane, the sphenoidal sinus is the most superior and posterior air space. In the more lateral plane, the sphenoidal sinus is situated more inferiorly, and the most posterosuperior air space is the posterior ethmoidal sinus. The sphenoidal sinus is usually embedded in the clivus and bordered superoposteriorly by the sella turcica. The ostium of the sphenoidal sinus lies in its anterosuperior region (Fig. 8). The sphenoidal sinus and the posterior ethmoid air cells drain into the superior meatus via the sphenoethmoidal recess or into the supreme meatus through tiny ostia located just under the superior turbinate. The sphenoethmoidal recess lies between the anterior wall of the sphenoidal sinus and the posterior ethmoidal sinus cells. The posterior nasal septum is frequently pneumatized and always in communication with the sphenoidal sinus. These air spaces can be infected, and a mucocele may evolve. Horizontally situated "septations" in the sphenoidal sinus are actually bony separations between the posterior ethmoidal sinus and the sphenoidal sinus. These

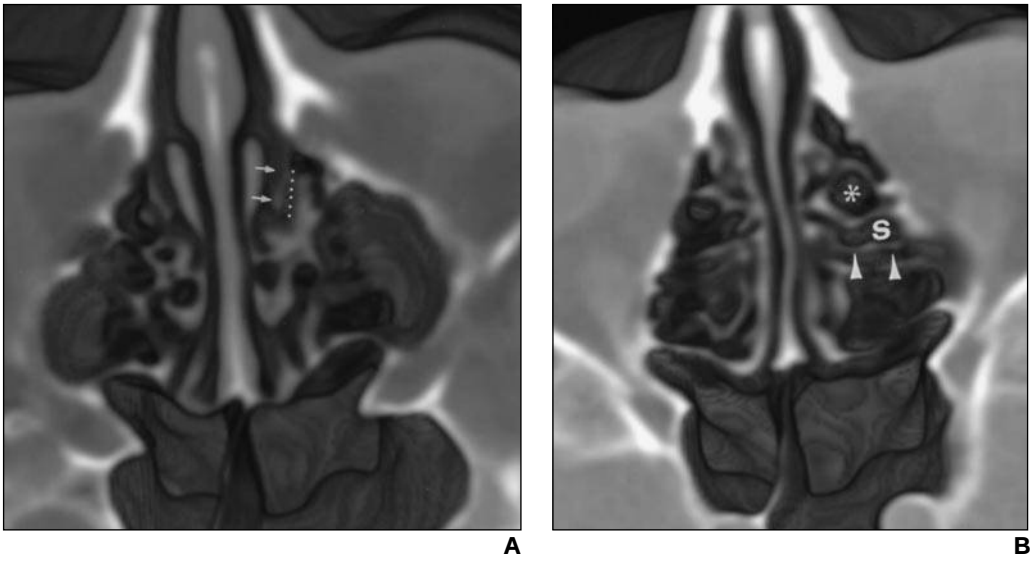

Fig. 6.—21-year-old woman with chronic sinus pain. Axial three-dimensional volume-rendered images obtained from helical CT data reveal anatomy of region of the basal lamella.
A, Image reveals location of uncinate process (*arrows*) and ethmoidal infundibulum (*dotted line*).
B, Image reveals location and orientation of retrobullar recess (s) situated between ethmoid bulla (*asterisk*) and basal lamella (*arrowheads*).

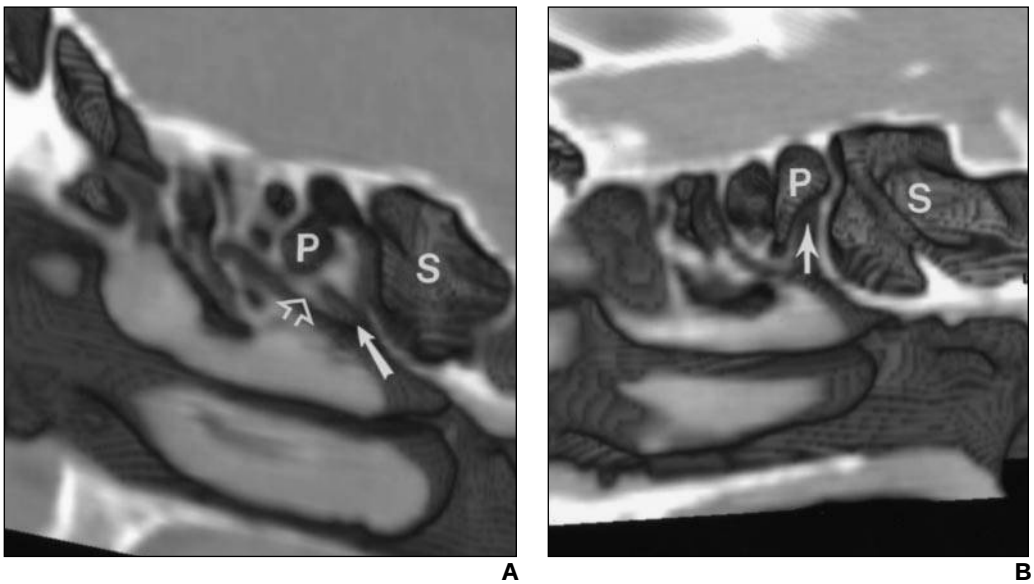

Fig. 7.—Sagittal three-dimensional volume-rendered images illustrate sphenoethmoidal recess region.
A, 53-year-old woman with facial pain. Image obtained from helical CT data reveals sphenoethmoidal recess (*solid arrow*), sphenoidal sinus (S), posterior ethmoidal sinus (P), and superior turbinate (*open arrow*).
B, 37-year-old man with sinus pain. Image shows sphenoethmoidal recess (*arrow*), sphenoidal sinus (S), and posterior ethmoidal sinus (P).

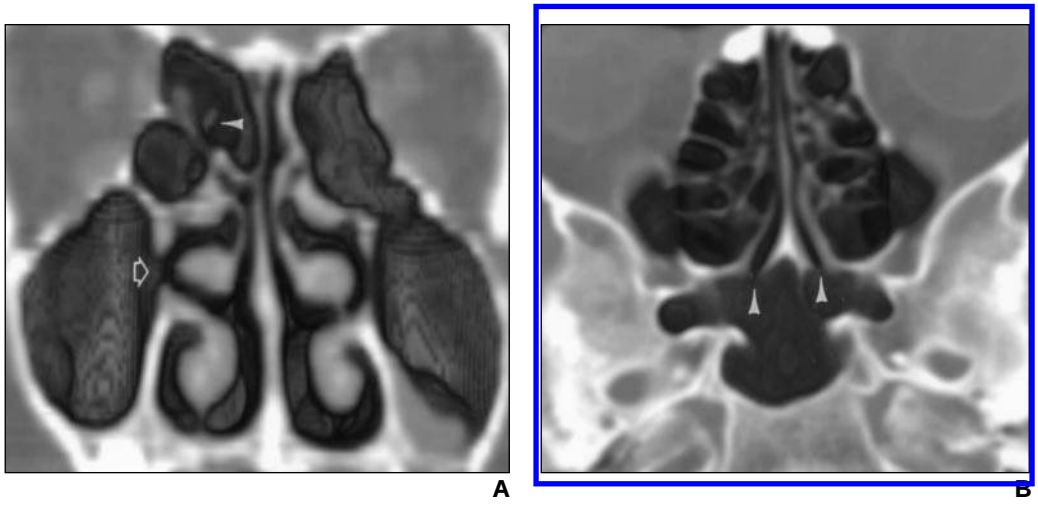

Fig. 8.—Three-dimensional volume-rendered images illustrate anatomy in the region of the sphenoidal sinus ostium.
A, 37-year-old man with sinus pain. Coronal image shows location of sphenoidal sinus ostium (*arrowhead*). Note dehiscence in medial maxillary sinus wall (*arrow*).
B, 43-year-old woman with sinus pain. Axial image shows sphenoidal sinus ostia (*arrowheads*).

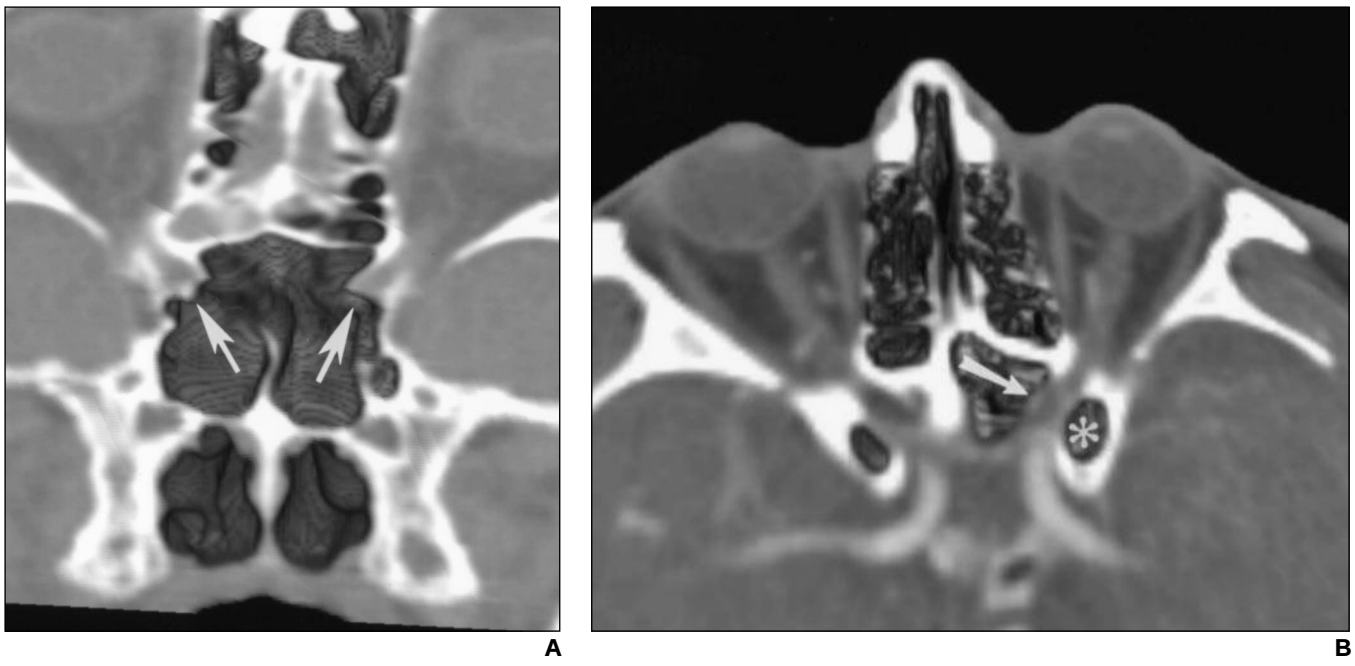

Fig. 9.—Three-dimensional volume-rendered images illustrate relationship of optic canal and carotid artery to sphenoidal sinus.
A, 37-year-old man with sinus pain. Axial image shows indentation of optic canal into sphenoidal sinus (*arrows*).
B, 32-year-old man with sinus pain. Oblique coronal image shows pneumatized anterior clinoid process (*asterisk*) and optic canal (*arrow*).

separations indicate a posterior extension of the posterior ethmoidal sinus above the aerated sphenoidal sinus. Septations in the sphenoidal sinus assume a vertical orientation. It is important to note whether these bony structures adhere to the carotid canal and optic canal. The surgeon operating in the sphenoidal sinus must be extremely careful not to infringe on this relationship (Fig. 9). Doing so could result in a carotid artery puncture or optic nerve injury [8].

References

1. Stammberger HR, Posawetz W. Functional endoscopic sinus surgery: concept, indications and results of the Messerklinger technique. *Eur Arch Otorhinolaryngol* **1990**;247:63–76
2. Zinreich SJ, Kennedy DW, Rosenbaum AE, Gayler BW, Kumar AJ, Stammberger HR. Paranasal sinuses: CT imaging requirements for endoscopic surgery. *Radiology* **1987**;163:769–775
3. Calhoun PS, Kuszyk BS, Heath DG, Carley JC, Fishman EK. Three-dimensional volume rendering of spiral CT data: theory and method. *RadioGraphics* **1999**;19:745–764
4. Rubin GD, Beaulieu CF, Agiro V, et al. Perspective volume rendering of CT and MR images: applications for endoscopic imaging. *Radiology* **1996**;199:321–330
5. Zinreich SJ, Mattox DE, Kennedy DW, Chisholm HL, Diffley DM, Rosenbaum AE. Concha bullosa: CT evaluation. *J Comput Assist Tomogr* **1988**;12:778–784
6. Yousern DM. Imaging of sinonasal disease. *Radiology* **1993**;188:303–314
7. Mafee MF, Chow JM, Meyers R. Functional endoscopic sinus surgery: anatomy, CT screening, indications, and complications. *AJR* **1992**;160:735–744
8. Van Alyea OE. Frontal cells: an anatomic study of these cells with consideration of their clinical significance. *Arch Otolargynol* **1941**;34:11–23
9. Schaeffer JP. The genesis, development, and adult anatomy of the nasofrontal region in man. *Am J Anat* **1916**;20:125–146
10. Hudgins PA, Browning DG, Gallups J, et al. Endoscopic paranasal sinus surgery: radiographic evaluation of severe complications. *AJNR* **1992**; 13:1161–1167